Electronic Supporting Information

Highly selective C_2H_2 and CO_2 capture based on two new Zn^{II}-MOFs and fluorescence sensing of two doped MOFs with Eu^{III}

Xin-Wei Meng,[a] Tao Ding,[*a] Bin Liu,[a] Xue-Song Gong,[a] Bo Liu,[a] and Li-Na Zheng[*a]

[a]School of Environmental and Chemical Engineering, Xi'an Polytechnic University,

Xi'an 710048, P. R China.

Table S1. Selected Bond Length (Å) and Angles (°) for **Zn-MOF 1-2**

Zn-MOF 1			
N11-Zn(1)-O14	101.1(9)	N11-Zn(1)-O54	103.3(9)
O14-Zn(1)-Zn(4)#1	73.7(5)	O14-Zn(1)-O54	81.8(10)
O54-Zn(1)-Zn(4)#1	76.5(5)	O25#2-Zn(1)-Zn(4)#1	79.7(6)
O25#2-Zn(1)-N11	100.8(9)	O25#2-Zn(1)-O14	96.6(11)
O25#2-Zn(1)-O54	155.7(8)	O25#2-Zn(1)-O65#2	75.4(11)
O65#2-Zn(1)-Zn(4)#1	80.1(7)	O65#2-Zn(1)-N11	105.0(10)
O65#2-Zn(1)-O14	153.6(9)	O65#2-Zn(1)-O54	95.2(9)
N31-Zn(3)-N23	103.3(10)	N31-Zn(3)-O35	95.2(11)
N23-Zn(3)-O35	121.4(10)	O85#3-Zn(3)-N31	110.1(13)
O85#3-Zn(3)-N23	116.4(12)	O85#3-Zn(3)-O35	107.8(11)
N21-Zn(2)-N33	106.9(10)	O34#4-Zn(2)-N21	113.7(12)
O34#4-Zn(2)-N33	110.9(11)	O84#2-Zn(2)-N21	112.0(11)
O84#2-Zn(2)-N33	104.8(9)	O84#2-Zn(2)-O34#4	108.1(9)
N13-Zn(4)-Zn(1)#5	175.2(7)	O24#5-Zn(4)-Zn(1)#5	82.1(6)
N13-Zn(4)-O24#5	101.1(8)	O24#5-Zn(4)-O64#5	93.6(11)
N13-Zn(4)-O64#5	102.8(9)	O24#5-Zn(4)-O15#6	83.0(10)
N13-Zn(4)-O15#6	98.6(9)	O24#5-Zn(4)-O55#6	160.3(8)
N13-Zn(4)-O55#6	98.5(9)	O64#5-Zn(4)-Zn(1)#5	80.4(6)
O15#6-Zn(4)-Zn(1)#5	78.2(6)	O64#5-Zn(4)-O55#6	82.8(11)
O15#6-Zn(4)-O64#5	158.5(8)	O15#6-Zn(4)-O55#6	93.3(10)
O55#6-Zn(4)-Zn(1)#5	78.3(6)		

Symmetrical codes: #1 x-1, y, z-1; #2 -x+1, y-1/2, -z; #3 -x+2, y-1/2, -z; #4 x, y, z+1; #5 x+1, y, z+1; #6 -x+2, y-1/2, -z+1; #7 x, y, z-1; #8 -x+1, y+1/2, -z; #9 -x+2, y+1/2, -z+1; #10 -x+2, y+1/2, -z for **Zn-MOF 1.**

Zn-MOF 2			
N(1)-Zn(1)-Zn(2)	180.0	N(2)-Zn(2)-Zn(1)	180.0
N(1)-Zn(1)-O(3)	99.8(6)	N(2)-Zn(2)-O(1)	102.4(7)
N(1)-Zn(1)-O(4)	100.0(6)	N(2)-Zn(2)-O(2)	98.7(7)

N(1)-Zn(1)-O(7)	99.4(7)	N(2)-Zn(2)-O(6)	101.4(7)
N(1)-Zn(1)-O(9)	103.1(6)	N(2)-Zn(2)-O(8)	101.4(7)
O(3)-Zn(1)-Zn(2)	80.2(6)	O(6)-Zn(2)-Zn(1)	78.6(7)
O(3)-Zn(1)-O(4)	76.5(6)	O(8)-Zn(2)-Zn(1)	80.4(6)
O(4)-Zn(1)-Zn(2)	80.0(6)	O(8)-Zn(2)-O(6)	77.2(8)
O(7)-Zn(1)-Zn(2)	80.6(7)	N(3)-Zn(3)-O(10)	60.9(4)
O(9)-Zn(1)-Zn(2)	76.9(6)	N(3)-Zn(3)-O(10)#2	61.1(4)
O(9)-Zn(1)-O(7)	76.9(7)	N(4)#1-Zn(3)-O(10)#2	62.1(4)
O(1)-Zn(2)-Zn(1)	77.6(7)	N(4)#1-Zn(3)-O(10)	63.1(4)
O(1)-Zn(2)-O(2)	79.2(7)	O(10)-Zn(3)-O(10)#2	77.6(4)
O(2)-Zn(2)-Zn(1)	81.3(7)		

Symmetrical codes: #1 x, -y+1/2, z+1/2, #2 -x+1, -y+1/2, z+0, #3 x, -y+1/2, z-1/2 for **Zn-MOF 2**

Table S2. A comparison of various MOF materials used for selective adsorption for C_2H_2 and CO_2 over CH_4

MOFs materials	IAST calculated selectivity		Ref.
	C_2H_2/CH_4	CO_2/CH_4	
$\{[Cu_4(L)_2(H_2O)_4]\cdot4DMF\cdot8H_2O\}_n$		3.2	43
ZJNU-63	13.1	3.5	44
Sc-ABTC	14.7		45
$\{[Co_6(\mu3\text{-}OH)4(Ina)_8](H_2O)_{10}(DMA)_2\}_n$	9.6		46
ZJU-16a	7.5		47
$\{[Zn_3(dbba)_2(bipy)(DMF)]\cdot3DMF\cdot4H_2O\}_n$		4	48
$\{[Co_3(L)(OH)_2(H_2O)_4]\cdot2DMF\cdot2H_2O\}_n$	13	4	49
SNNU-5-In	10	3.9	50
Zn-MOF 1	15.1	6.8	This work
Zn-MOF 1	14.2	6.5	This work

Table S3 Comparison the Ksv of **Eu@Zn-MOF 1** and **Eu@Zn-MOF 2** towards Fe^{3+} ions with other materials.

Materials	Solvent	Ksv (M^{-1})	Ref.
Bis(rhodamine)-1	CH_3CN	7.50×10^3	51
Bis(rhodamine)-2	CH_3CN	5.10×10^3	51
BUT-14	H_2O	2.17×10^3	52
BUT-15	H_2O	1.66×10^4	52
Eu^{3+}@MIL-53-COOH (Al)	H_2O	5.12×10^3	53
Ln(cpty)3	H_2O	4.10×10^3	54
Benzimidazole-based sensor	H_2O	8.51×10^4	55
FJU-13a-Eu	H_2O	2.03×10^4	56
$Eu_2(MFDA)_2(HCOO)_2(H_2O)_6$	DMF	1.58×10^3	57

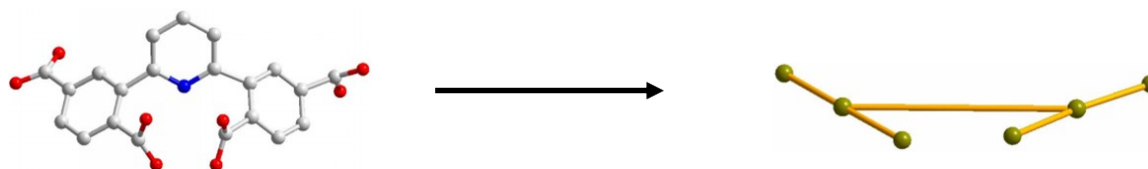| Tb-DSOA	H_2O	3.54×10^3	58
Eu(atpt)1.5(phen)(H2O)	CH_3CH_2OH	7.60×10^3	59
Eu@Zn-MOF 1	H_2O	1.53×10^4	This work
Eu@Zn-MOF 2	H_2O	1.43×10^4	This work

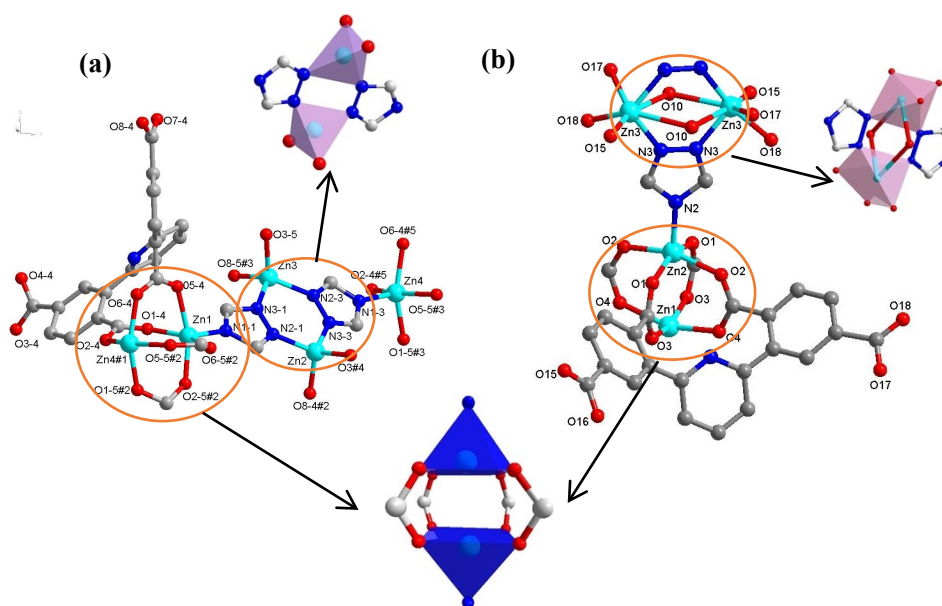**Figure S1.** The L^{4-} ligand viewed as two 3-c nodes.

Figure S2. Single-crystal structure of 1. (a) Coordination environments of Zn ions in **Zn-MOF 1**.The hydrogen atoms are omitted for clarity. #1 x-1, y, z-1; #2 -x+1, y-1/2, -z; #3 -x+2, y-1/2 ,-z; #4 x, y, z+1; #5 x+1, y, z+1; (b) Coordination environments of Zn ions in **Zn-MOF 2**.The hydrogen atoms are omitted for clarity.#1 x, -y+1/2, z+1/2 #2 -x+1, -y+1/2, z+0 #3 x, -y+1/2, z-1/2.
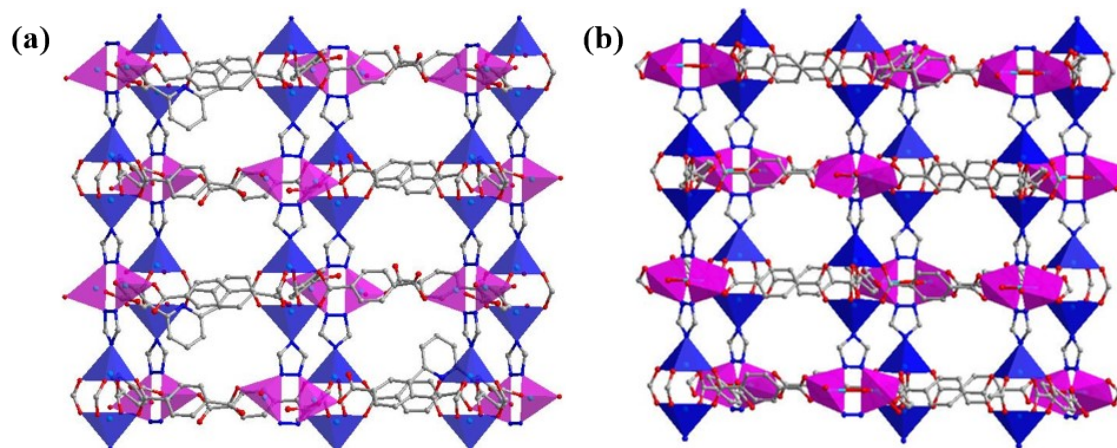
Figure S3. 2D double-layer of **Zn-MOF 1** (a), **Zn-MOF 2** (b).
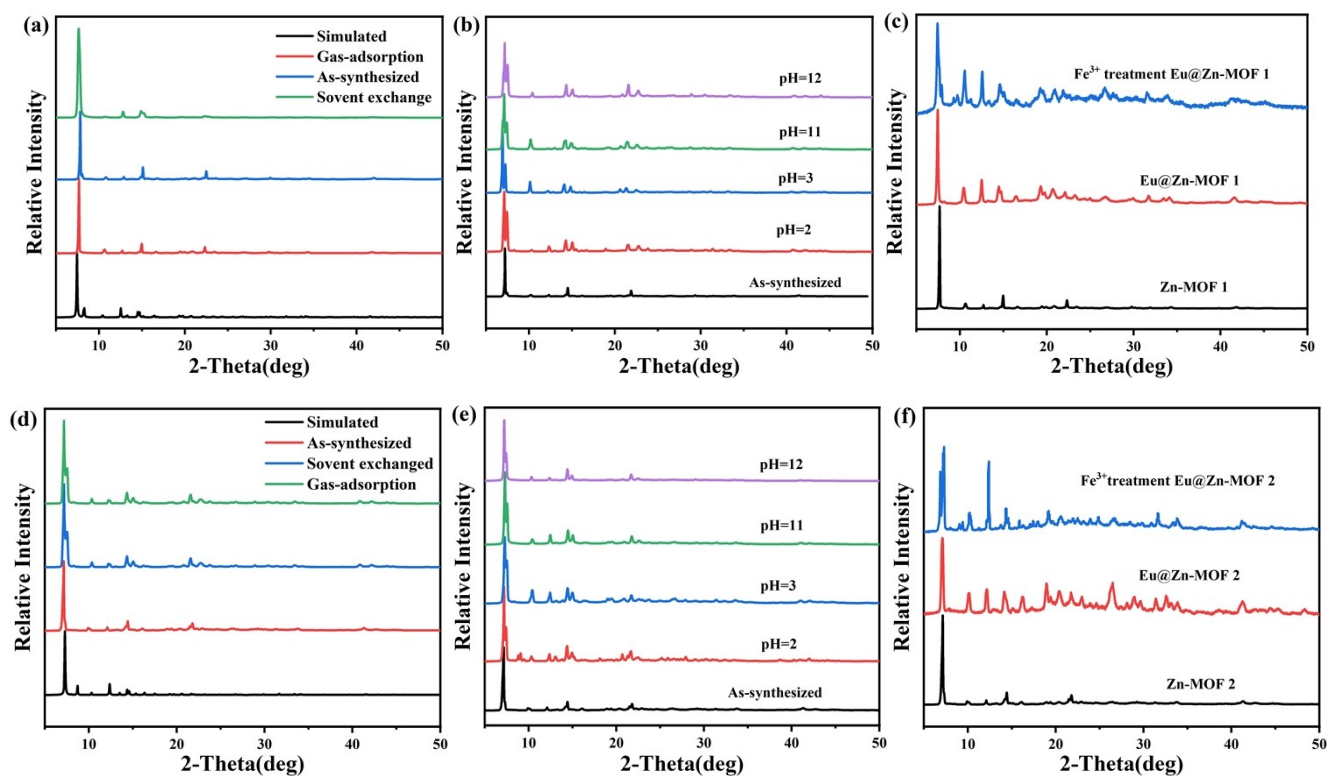
Figure S4. PXRD patterns. Simulated, as-synthesized, Gas-adsorption and Solvent exchanged of **Zn-MOF 1** (a) and **Zn-MOF 2** (d). After being soaked in acidic and basic solutions for different time periods of **Zn-MOF 1** (b) and **Zn-MOF 2** (e). Before and after immersion in $Fe^{3+}$of **Eu@Zn-MOF 1** (c) **and Eu@Zn-MOF 2** (f).
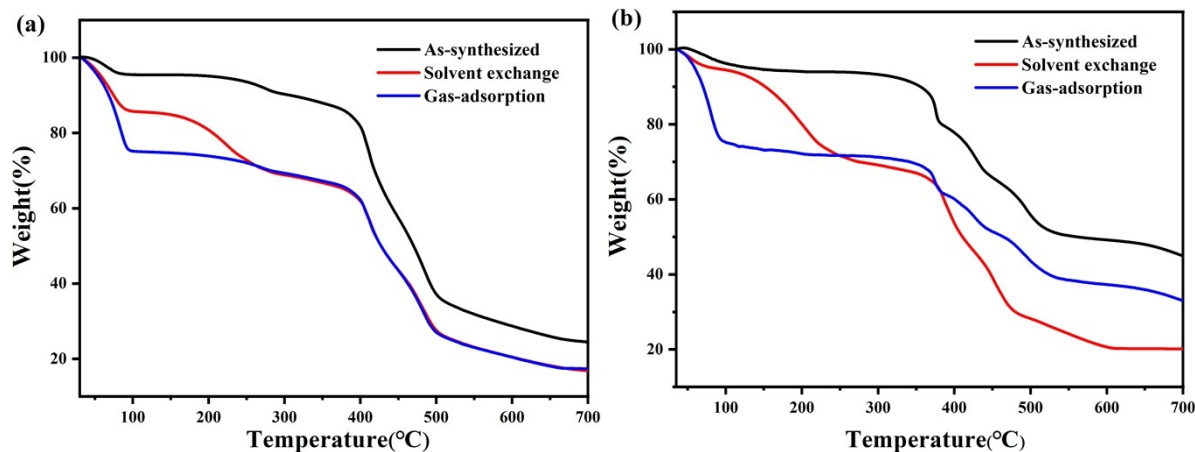
Figure S5. TGA for **Zn-MOF 1** (a) and **Zn-MOF 2** (b): As-synthesized, exchanged and Gas-adsorption samples.
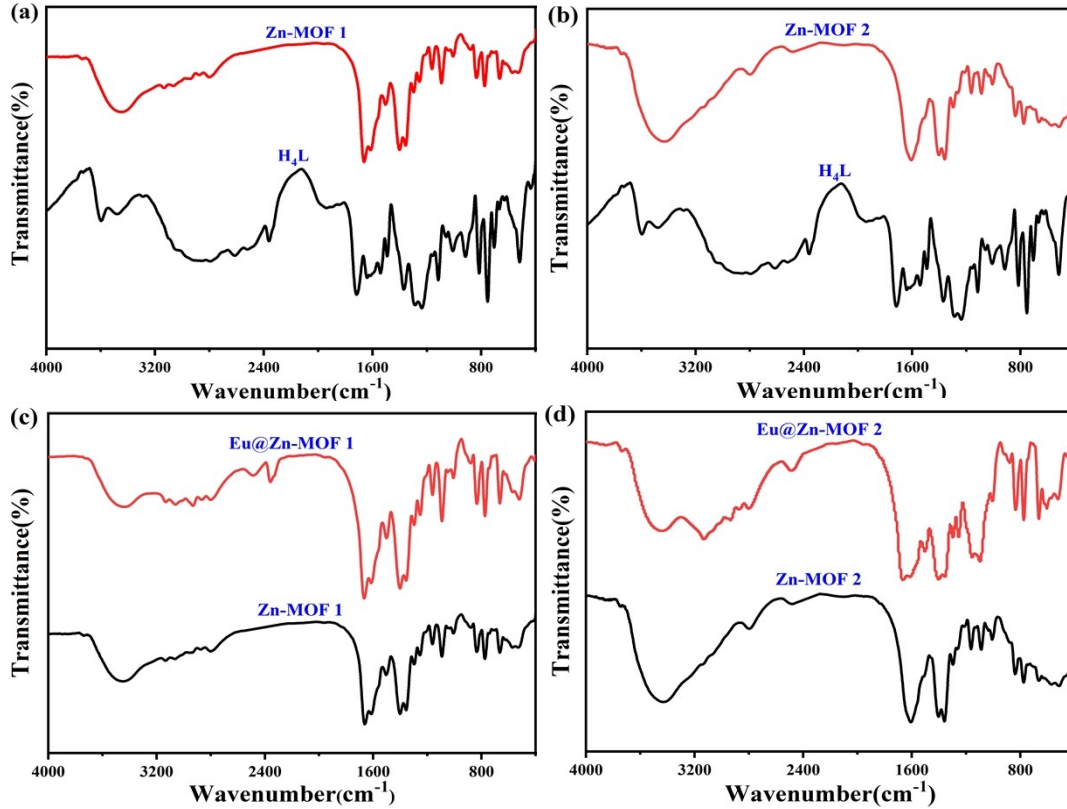
Figure S6. IR for (a) **Zn-MOF 1**, (b) **Eu@Zn-MOF 1**, (c) **Zn-MOF 2**, (d) **Eu@Zn-MOF 2**: ligand and as-synthesized samples.

IAST adsorption selectivity calculation

The experimental isotherm data for pure CO_2, CH_4 and C_2H_2 (measured at 298 K) were fitted using a Langmuir-Freundlich (L-F) model.

$$q = \frac{a \times b \times p^c}{1 + b \times p^c}$$

Where q and p are adsorbed amounts and pressures of component i, respectively. The adsorption selectivities for binary mixtures of CO_2/CH_4 at 273 and 298 K and C_2O_2/CH_4 at 298K, defined by

Where qi is the amount of i adsorbed and pi is the partial pressure of i in the mixture.

$$S_{ads} = \frac{q_1/q_2}{p_1/p_2}$$

Figure S7. (a) The consistency plot, (c) BET surface area plot, and (e) Langmuir surface area plot for **Zn-MOF 1**, (b) The consistency plot, (d) BET surface area plot, and (f) Langmuir surface area plot for **Zn-MOF2**.
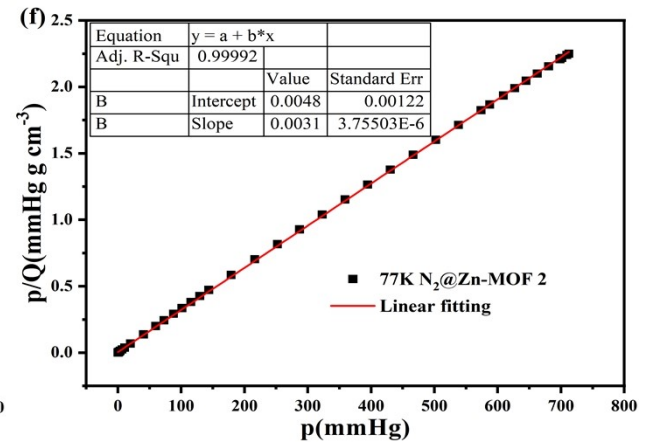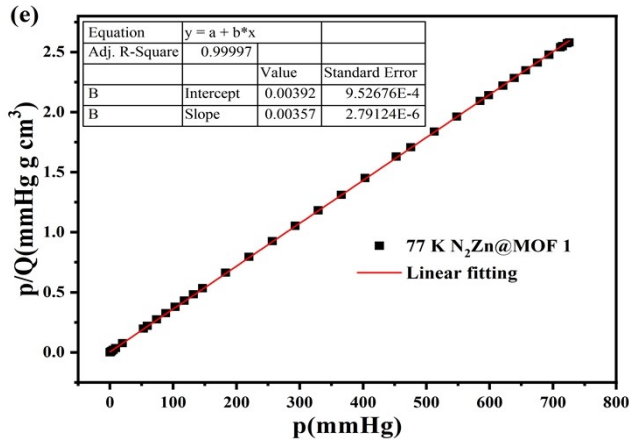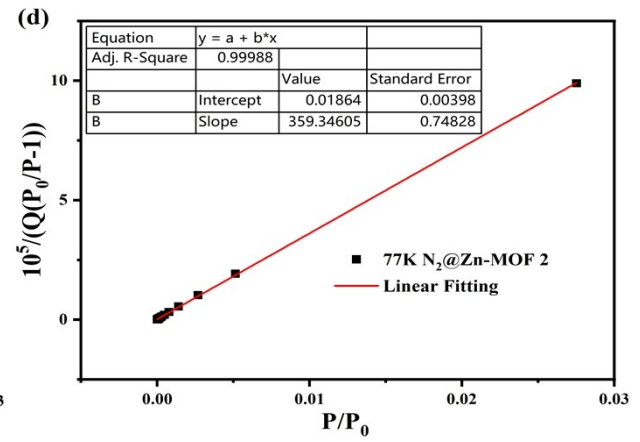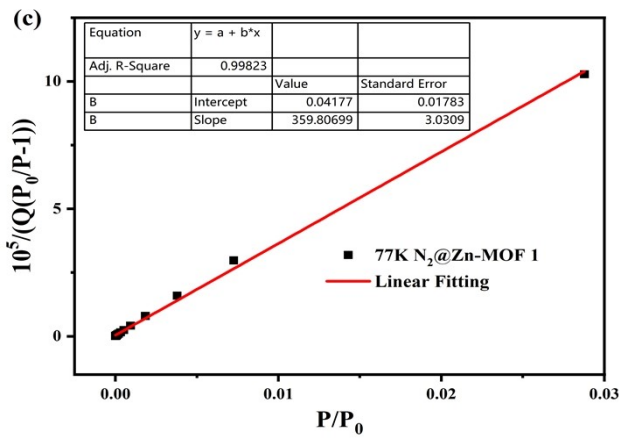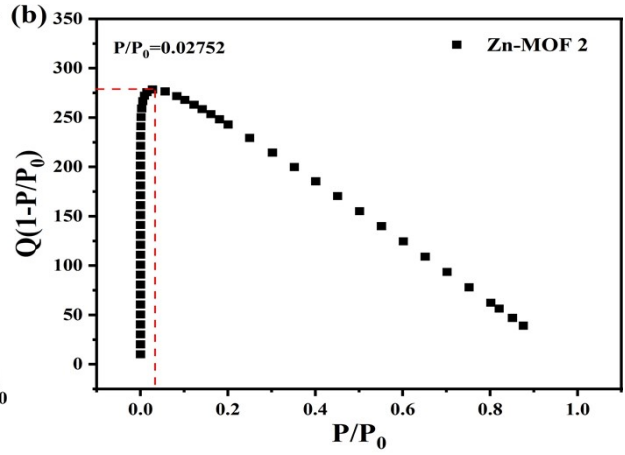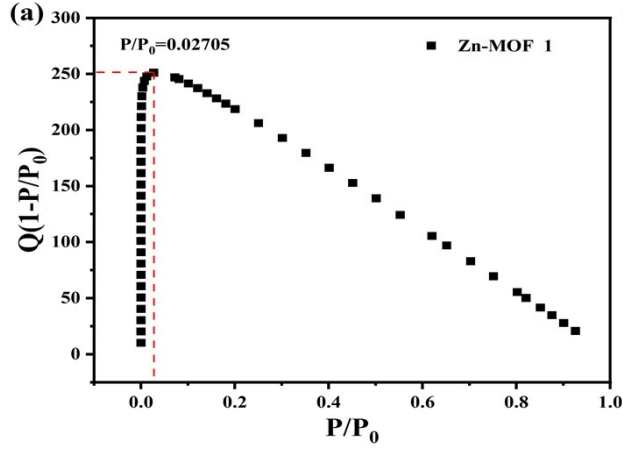
$S_{BET}=1/(0.042\times10^{-6}+359.82)\times10^5/22414\times6.023\times10^{23}\times0.162\times10^{-18}=1209.83$ m^2 g^{-1}

$S_{Langmuir}=(1/0.00357)/22414\times6.023\times10^{23}\times0.162\times10^{-18}=1219.38$ m^2 g^{-1}

BET constant $C=1+359.81/0.042\times10^5\times10^{-6}=857.69$

$$(P/P_0)_{nm}=\frac{1}{\sqrt{C}+1}=0.033018$$

$S_{BET}=1/(0.019\times10^{-6}+359.35)\times10^5/22414\times6.023\times10^{23}\times0.162\times10^{-18}=1211.41$ m^2 g^{-1}

$S_{Langmuir}=(1/0.0031)/22414\times6.023\times10^{23}\times0.162\times10^{-18}=1404.27$ m^2 g^{-1}

BET constant C$=1+359.35/0.042\times10^5\times10^{-6}=856.60$
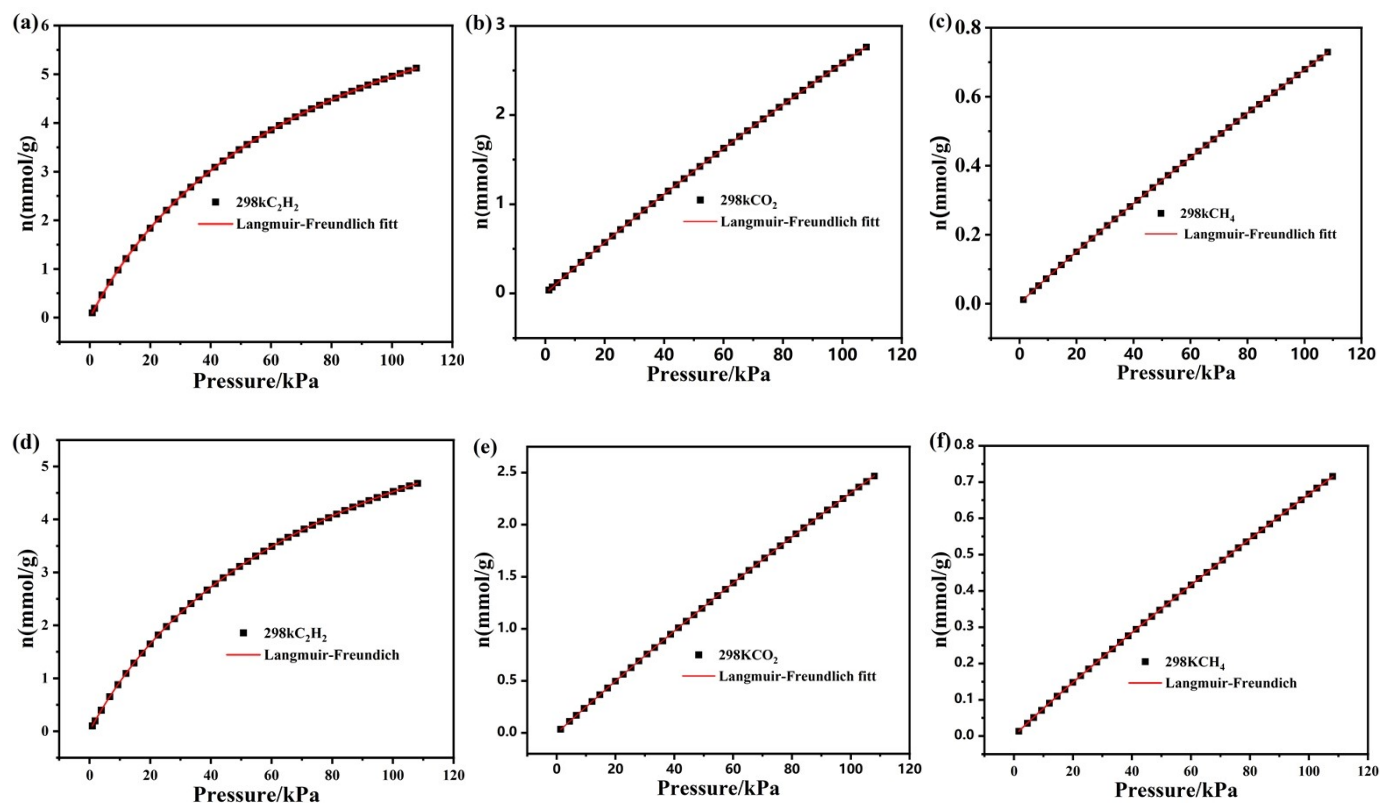
$$(P/P_0)_{nm}=\frac{1}{\sqrt{C}+1}=0.032983$$

Figure S8. (a) C$_2$H$_2$ adsorption isotherms of **Zn-MOF 1** at 298 K with fitting by L-F model: a =8.84199, b =0.01393, c =0.01892, Chi^2 = 5.41538E-6, R^2 = 1.00000; (b) CO$_2$ adsorption isotherms of **Zn-MOF 1** at 298 K with fitting by L-F model: a =23.4444, b =0.00127, c =0.00587, Chi^2 =2.36173E-6, R^2 = 1.00000; (c) CH$_4$ adsorption isotherms of **Zn-MOF 1** at 298 K with fitting by L-F model: a = 13.12646, b =6.55114E-4, c =0.04004, Chi^2 = 2.72873E-7, R^2 =0.9999; (d) C$_2$H$_2$ adsorption isotherms of **Zn-MOF 2** at 298 K with fitting by L-F model: a =8.4592, b =0.01342, c =0.0337, Chi^2 = 3.49595E-6, R^2 = 1.00000; (e) CO$_2$ adsorption isotherms of **Zn-MOF 2** at 298 K with fitting by L-F model: a =21.34253, b =0.00116, c =-0.00884, Chi^2 =1.6233E-6, R^2 = 1.00000; (f) CH$_4$ adsorption isotherms of **Zn-MOF 2** at 298 K with fitting by L-F model: a = 12.09448, b =6.88961E-4, c =0.03614, Chi^2 = 1.10292E-7, R^2 =1.0000;

Calculation of sorption heat for C$_2$H$_2$ and CO$_2$ uptakes using Virial 2 model

The above equation was applied to fit the combined C$_2$H$_2$ and CO$_2$ and isotherm data for desolvated 1 at

273 and 298 K, where P is the pressure, N is the adsorbed amount, T is the temperature, ai and bi are virial coefficients, and m and n are the number of coefficients used to describe the isotherms. Q_{st} is the coverage-dependent enthalpy of adsorption and R is the universal gas constant.

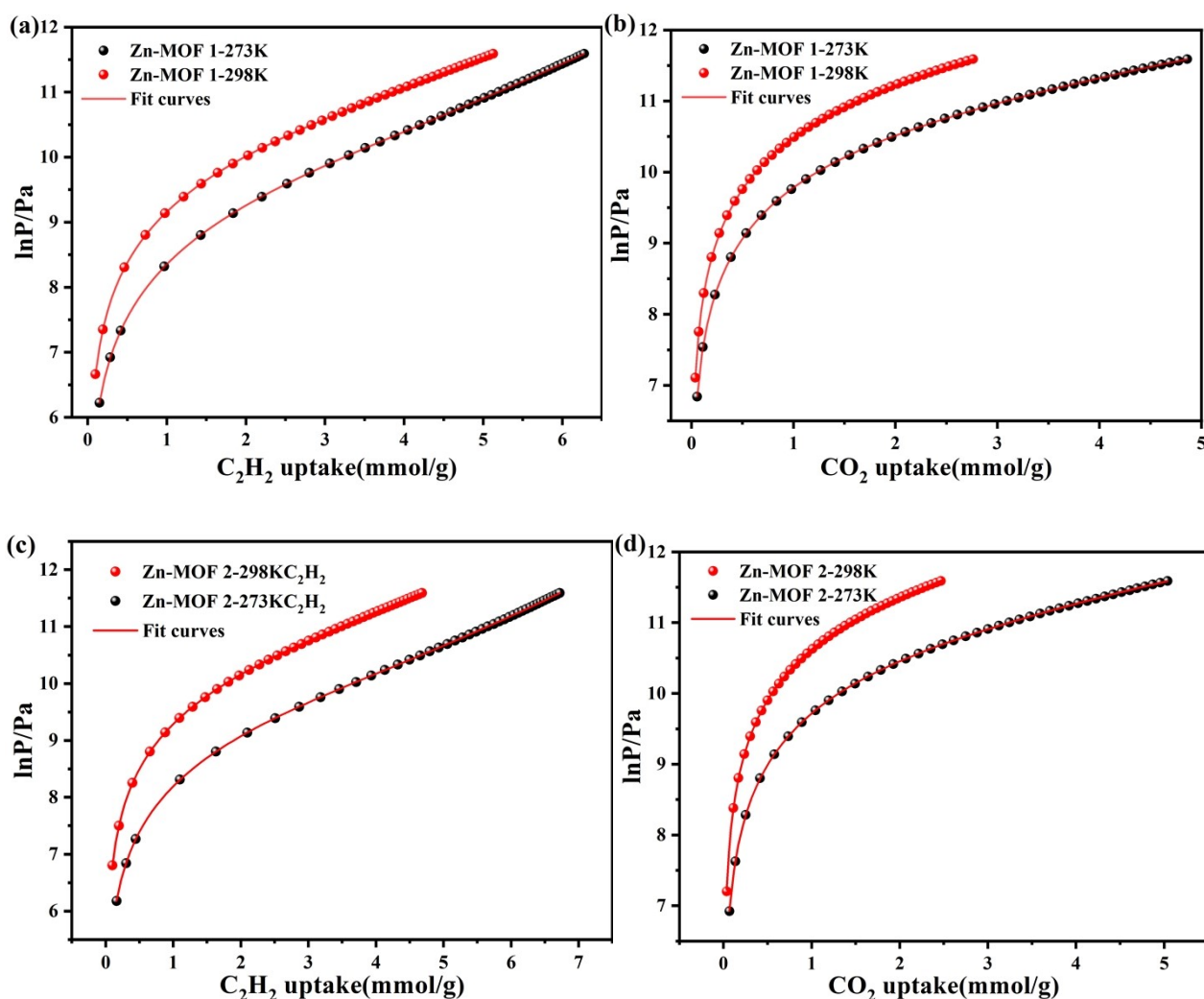$$lnp = lnN + 1/T \sum_{i=0}^{m} a_i N^i + \sum_{i=0}^{n} b_i N^i \quad Q_{st} = -R \sum_{i=0}^{m} a_i N^i$$

Figure S9. (a) Virial analysis of the C_2H_2 adsorption data at 298 K and 273 K for **Zn-MOF 1**. Fitting results:

A0 = -2862.81452, A1 = 286.59277, A2 = -55.76345, A3 =6.96046, A4 = -0.15284, Chi^2 = 5.35045E-6, R^2 = 1, B0=18.5486, B1 = -0.74012, B2 = 0.14685, B3 =-0.01399; (b) Virial analysis of the CO2 adsorption data at 298 K and 273 K for **Zn-MOF 1**. Fitting results: A0= -2170.06756, A1= -254.82424, A2 = 154.06248, A3 =-30.59728, A4 = -0.25843, Chi^2 = 2.30489E-5, R^2 = 0.99998 B0=17.66738, B1 = 1.02847, B2 = -0.60576, B3 =0.12369; (c) Virial analysis of the C_2H_2 adsorption data at 298 K and 273 K for **Zn-MOF 2**. Fitting results: A0= -3647.84636, A1 = 117.62901, A2 = -37.56691, A3 =4.22109, A4

= -0.09628, Chi^2 = 5.97073E-6, R^2 = 1; B0= 21.32644, B1 = -0.16174, B2 = 0.09364, B3 =-0.00673,(d)
Virial analysis of the CO2 adsorption data at 298 K and 273 K for **Zn-MOF 2**. Fitting results: A0=
3023.00731, A1= -83.10174, A2 = -7.2069, A3 =12.87007, A4 = -0.34707, Chi^2 = 1.54628E-5, R^2 =
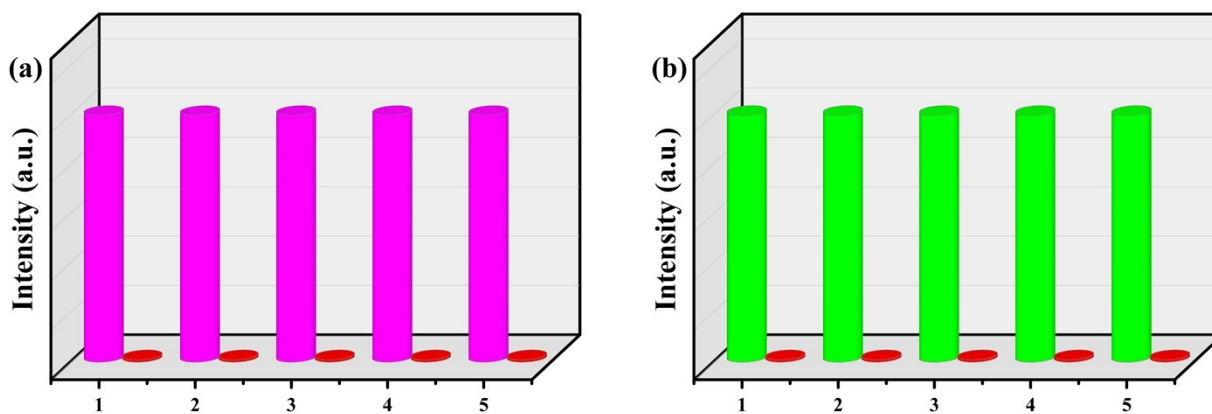0.99999 B0= -0.51505, B1 = 0.4125, B2 = -0.03495, B3 =-0.02818

Figure S10. Comparison of fluorescence properties of **Eu@Zn-MOF 1** (a) and **Eu@Zn-MOF 2** (b)
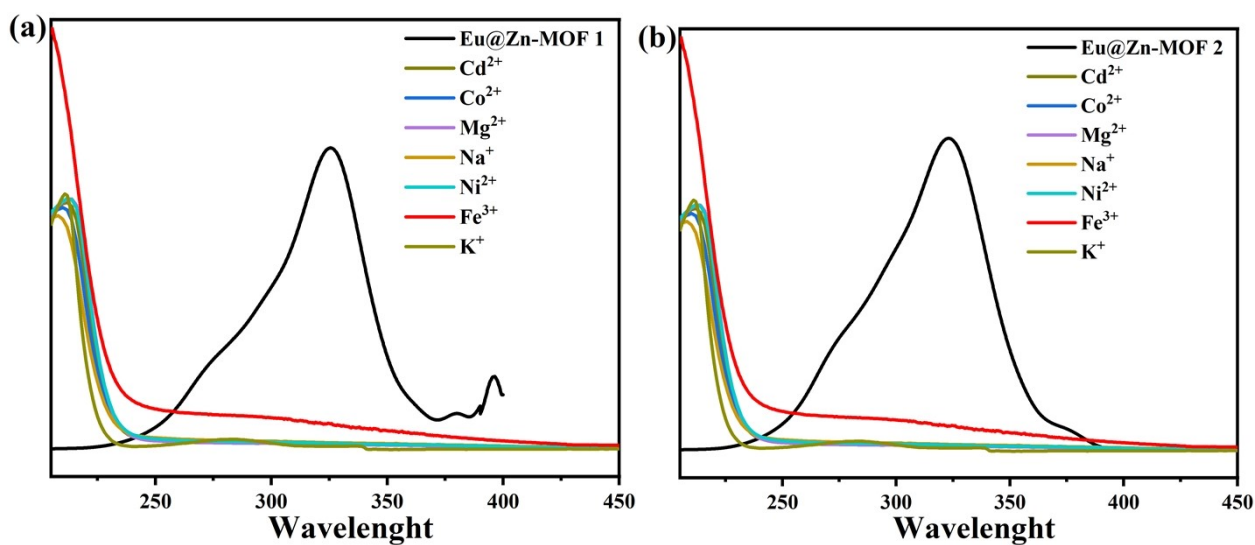before and after recovery.

Figure S11. UV-vis adsorption spectra of $M(NO_3)_x$ aqueous solutions and the excitation spectrum of
Eu@Zn-MOF 1 (a) and **Eu@Zn-MOF 2** (b).

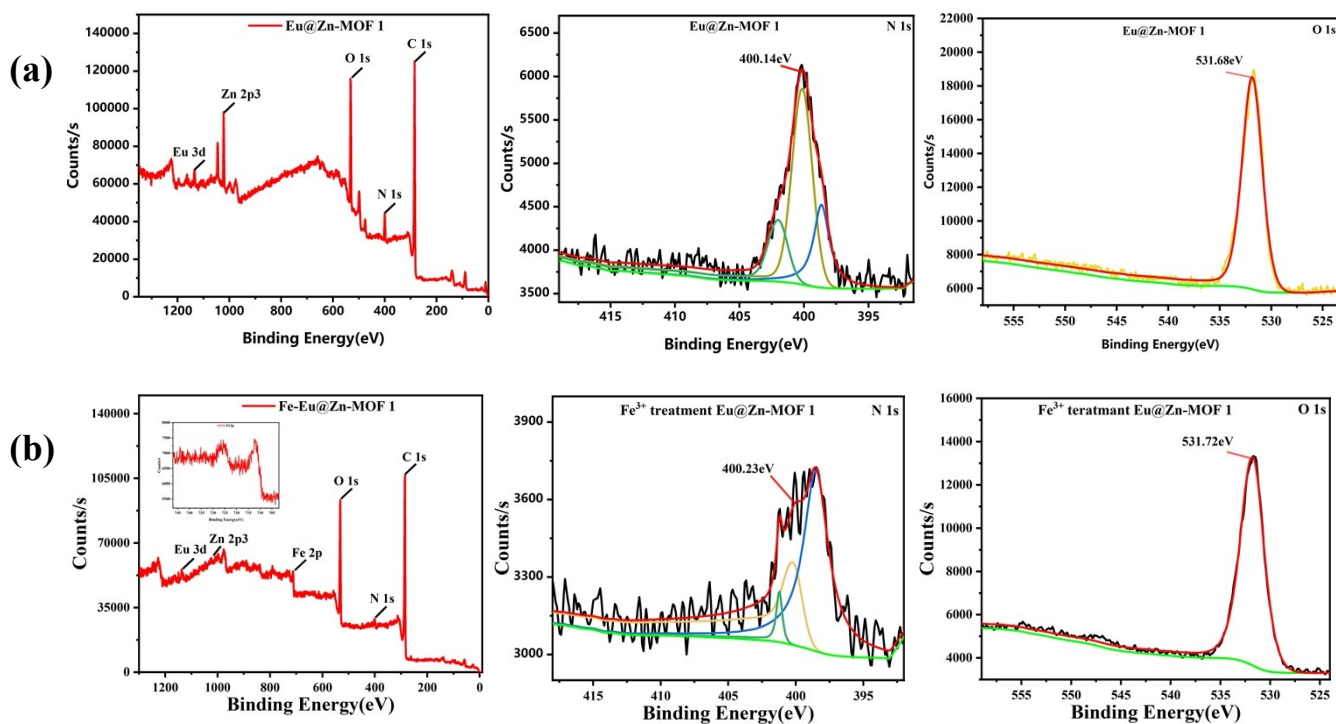**Figure S12.** Comparison of the XPS spectra of **Eu@Zn-MOF 1** before (a) and after (b) treatment with Fe^{3+} ions: overall spectra (left); N1s (middle); O1s(right).
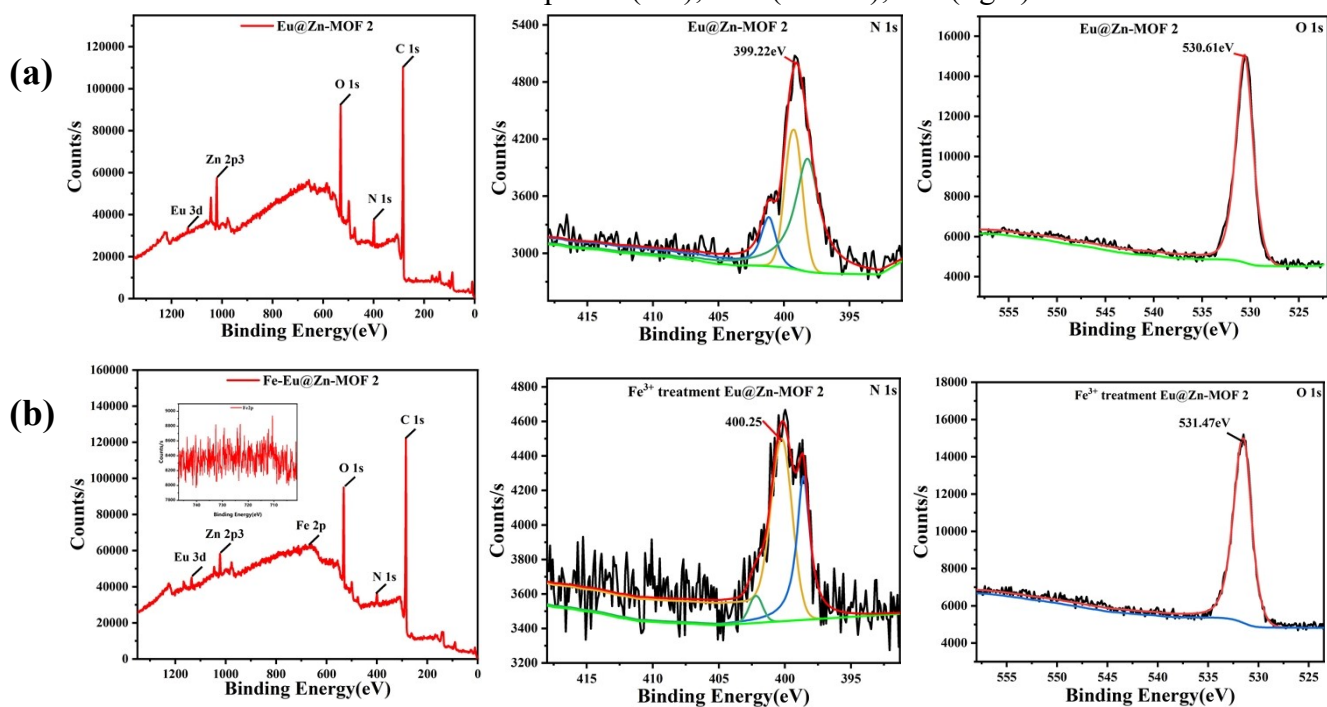
Figure S13. Comparison of the XPS spectra of **Eu@Zn-MOF 2** before (a) and after (b) treatment with Fe^{3+} ions: overall spectra (left); N1s (middle); O1s (right)